

This is an Open Access document downloaded from ORCA, Cardiff University's institutional repository: <https://orca.cardiff.ac.uk/id/eprint/123143/>

This is the author's version of a work that was submitted to / accepted for publication.

Citation for final published version:

Beltrachini, Leandro 2019. The analytical subtraction approach for solving the forward problem in EEG. *Journal of Neural Engineering* 16 (5) , 056029. 10.1088/1741-2552/ab2694

Publishers page: <http://dx.doi.org/10.1088/1741-2552/ab2694>

Please note:

Changes made as a result of publishing processes such as copy-editing, formatting and page numbers may not be reflected in this version. For the definitive version of this publication, please refer to the published source. You are advised to consult the publisher's version if you wish to cite this paper.

This version is being made available in accordance with publisher policies. See <http://orca.cf.ac.uk/policies.html> for usage policies. Copyright and moral rights for publications made available in ORCA are retained by the copyright holders.



Supplementary material to the manuscript
“The analytical subtraction approach for solving the forward problem
in EEG”

Submitted to Journal of Neural Engineering

L. Beltrachini

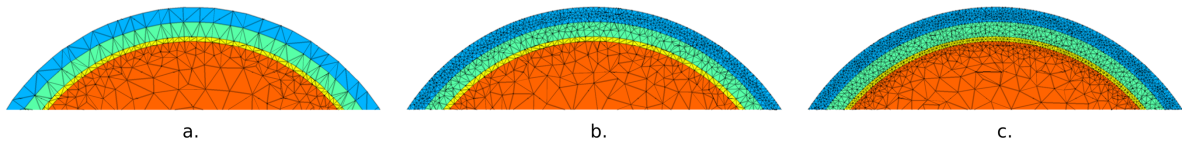


Figure S1.1 Detail of three (out of six) spherical head models utilised for the simulations. a. 39k nodes. b. 281k nodes. c. 640k nodes.

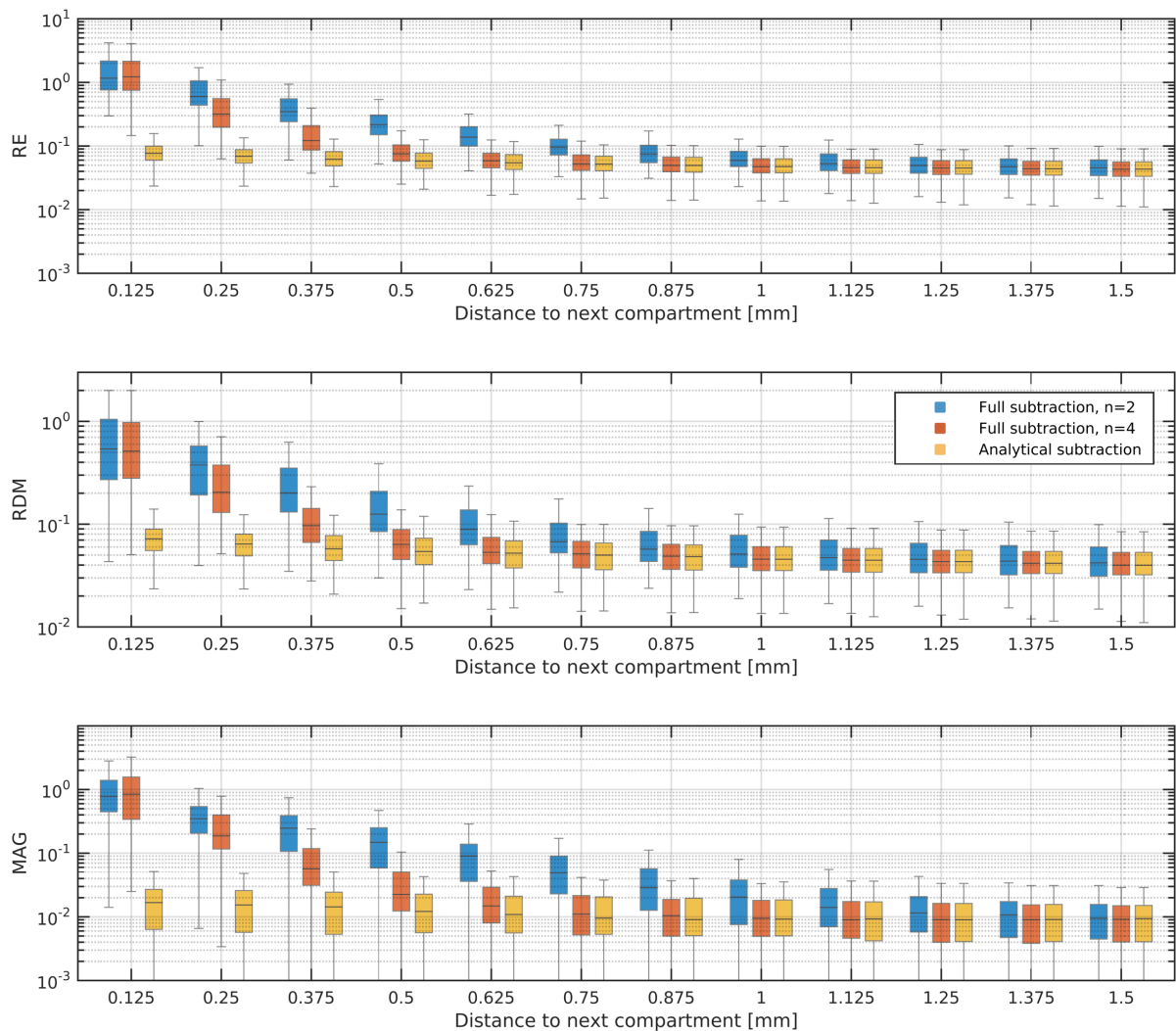


Figure S1.2 Error! No text of specified style in document. Error measures (RE: top; RDM: centre; MAG: bottom) for the numerical solutions of the EEG-FP as a function of the distance to the next compartment considering tangentially-oriented sources and the model with 39k nodes. Results are presented for the AS and FS (n=2 and n=4) methods (with different colours).

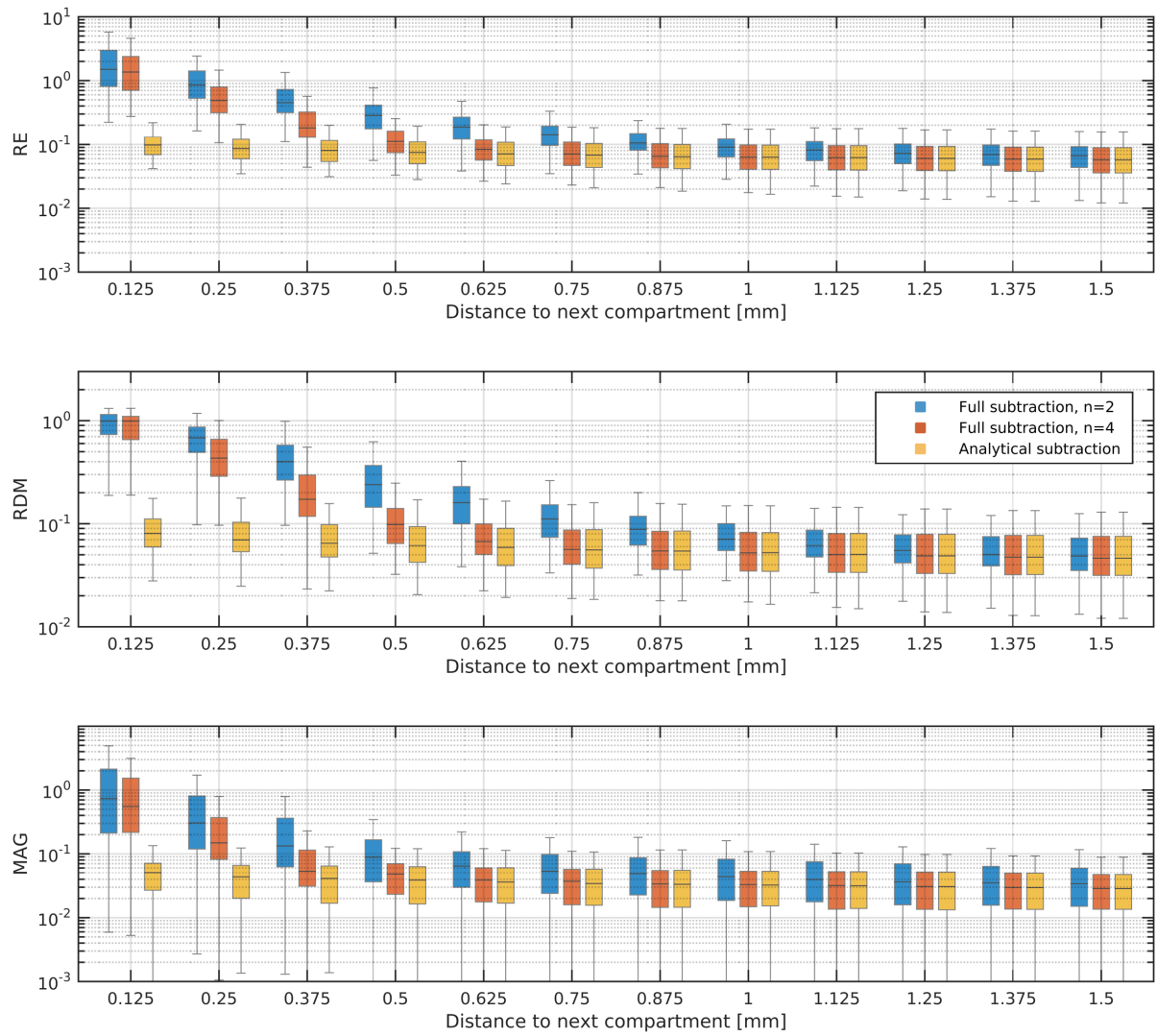


Figure S1.3 Idem Figure S1.2 for radially-oriented sources.

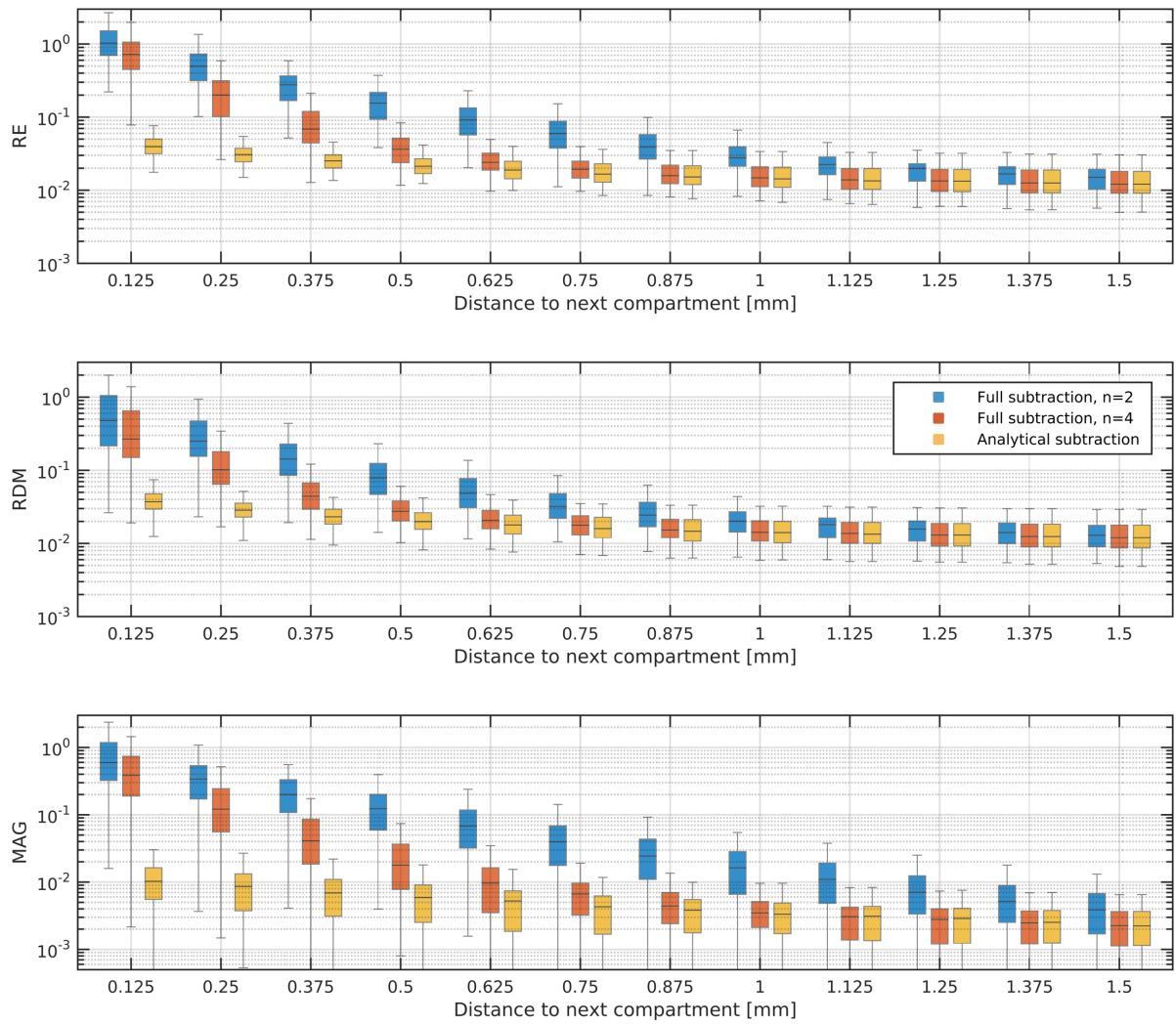


Figure S1.4 Idem Figure S1.2 for the model with 119k nodes.

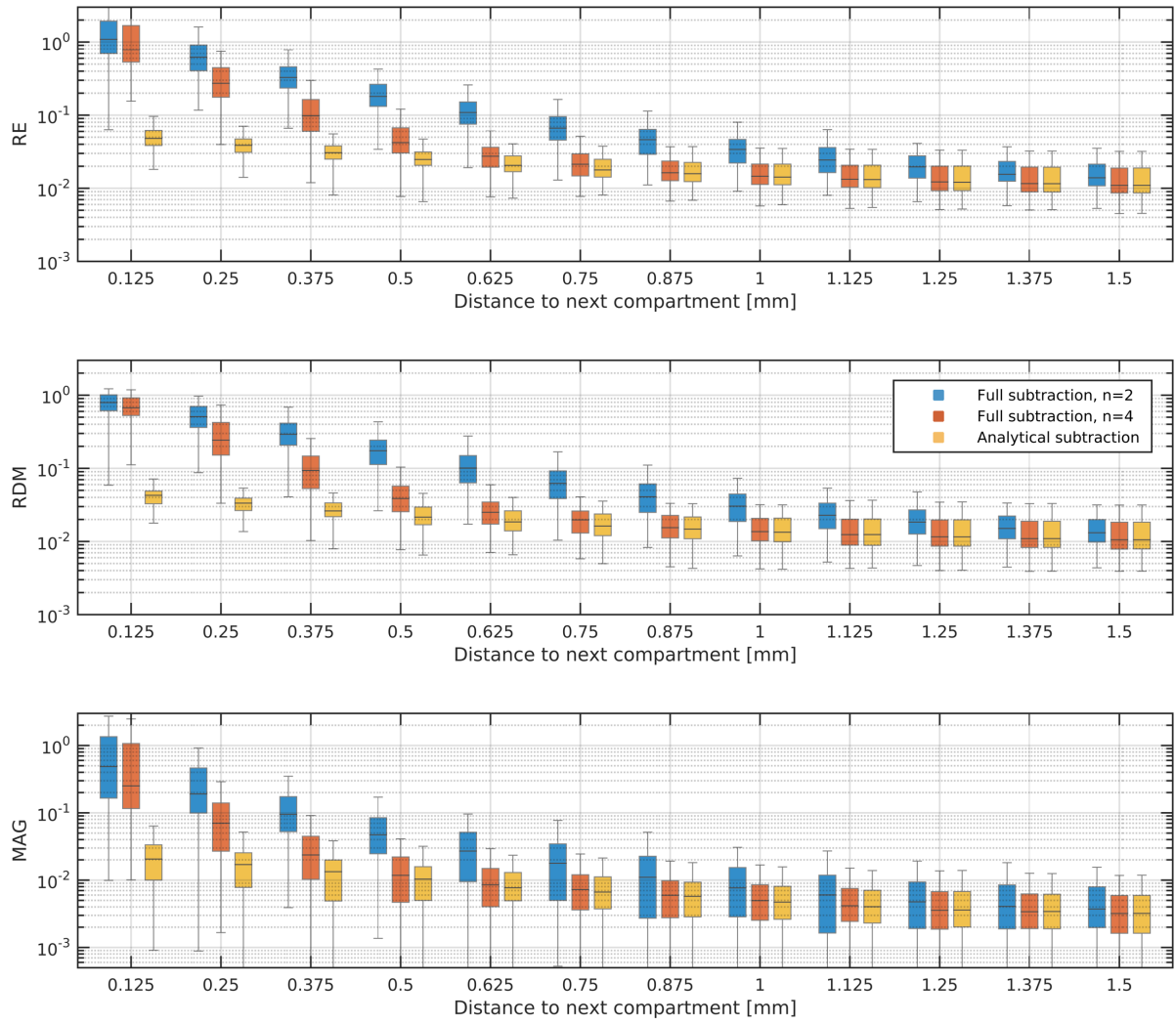


Figure S1.5 Idem Figure S1.3 for the model with 119k nodes.

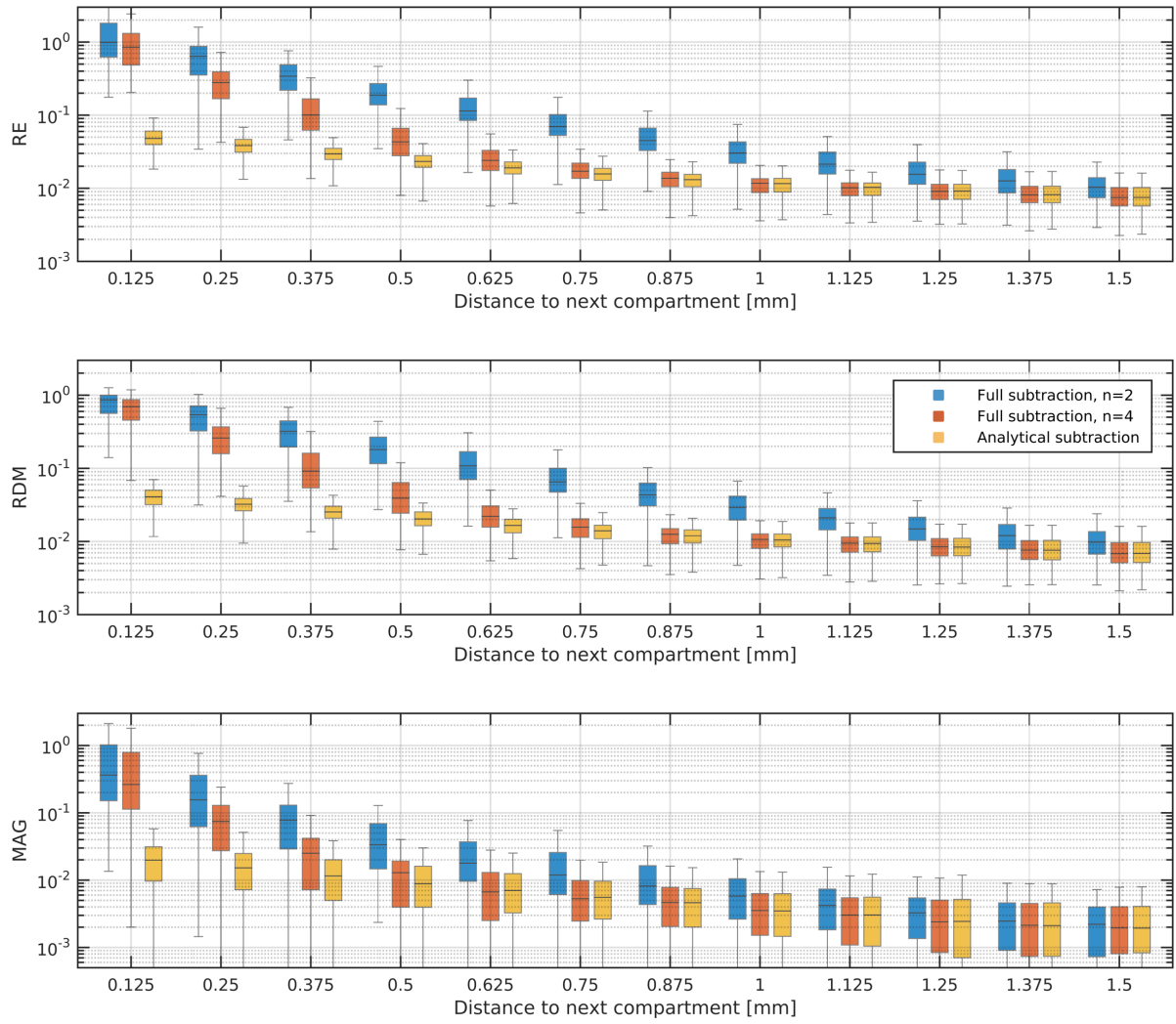


Figure S1.6 Idem Figure S1.3 for the model with 281k nodes.

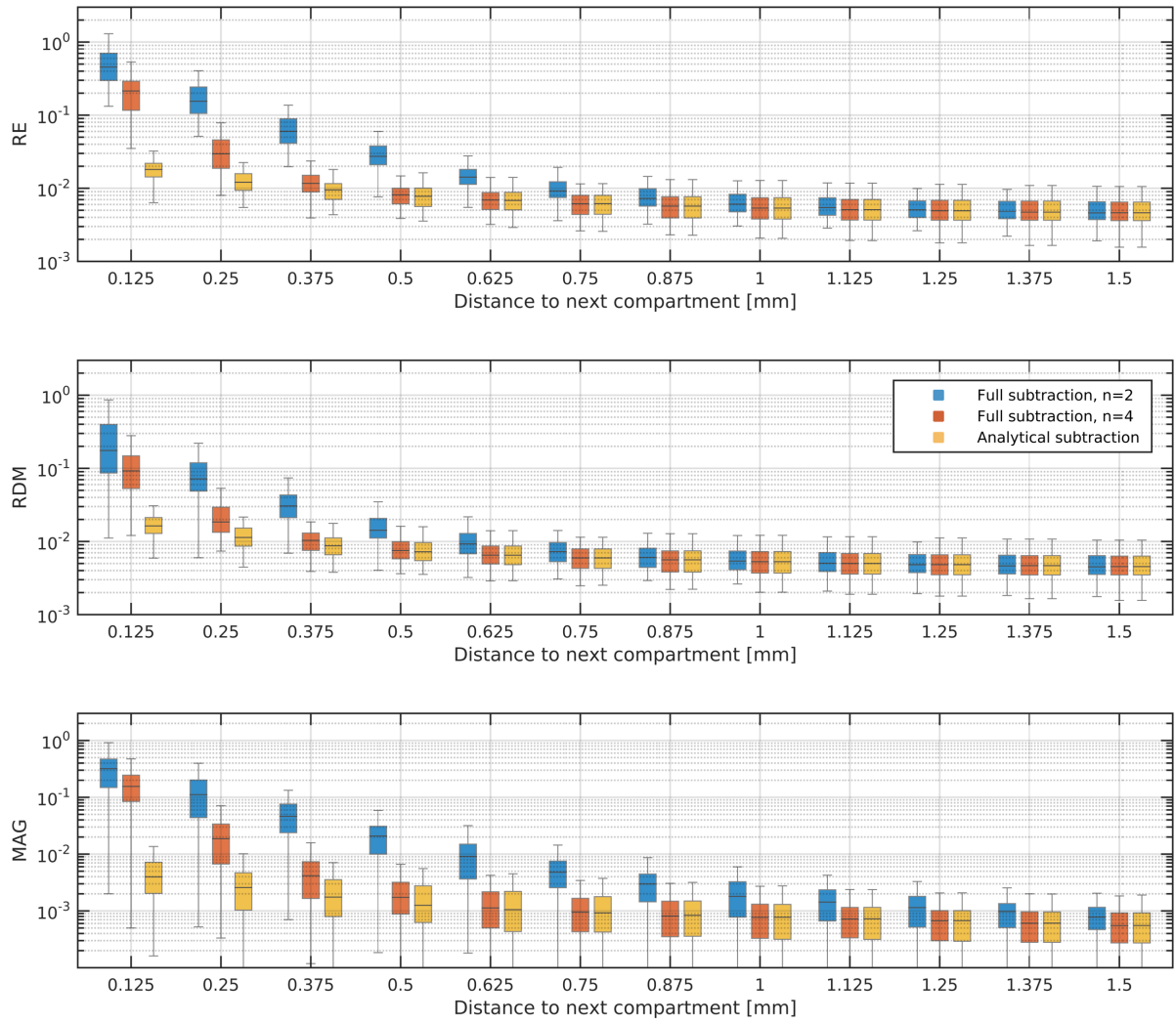


Figure S1.7 Idem Figure S1.2 for the model with 440k nodes.

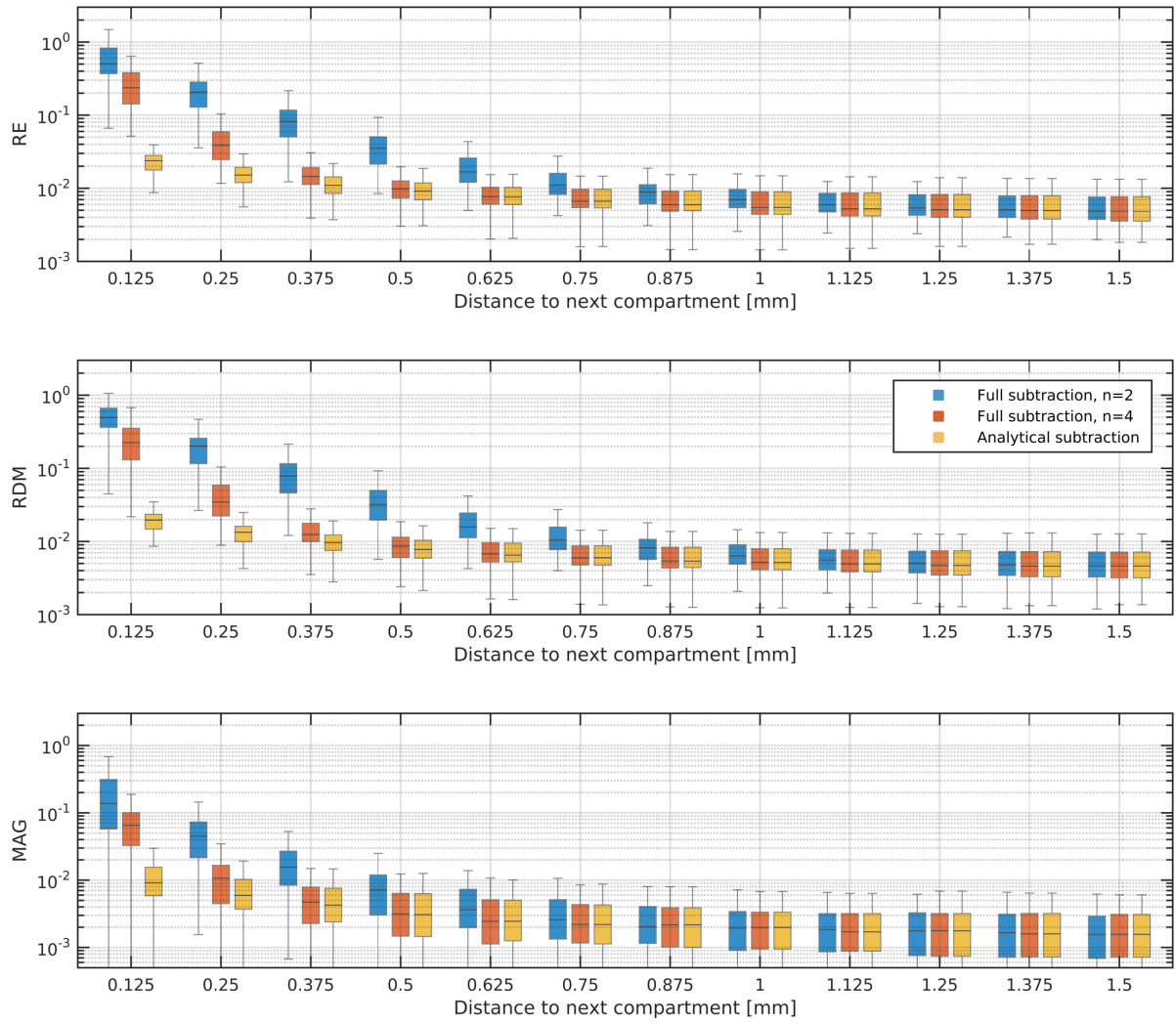


Figure S1.8 Idem Figure S1.3 for the model with 440k nodes.

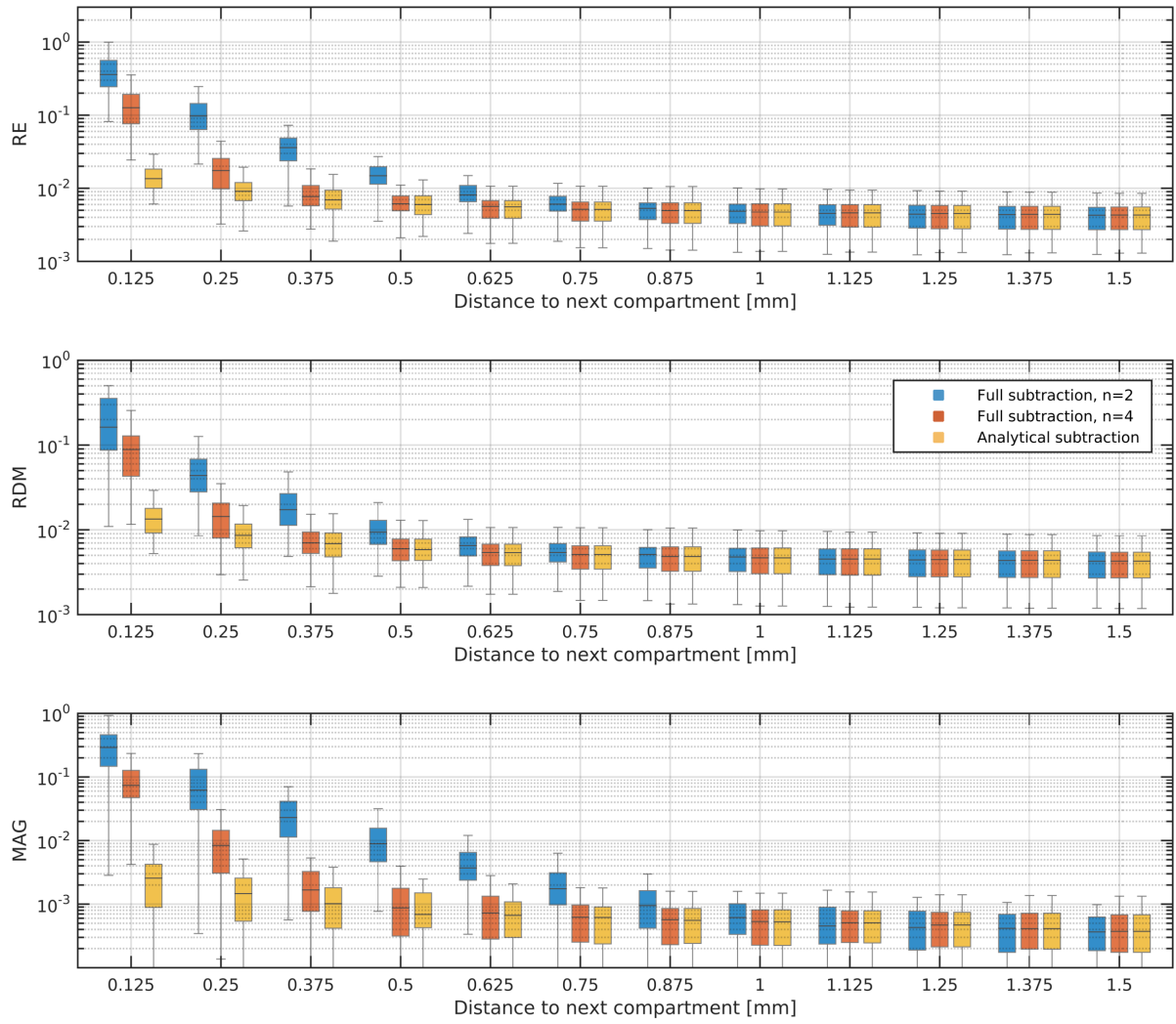


Figure S1.9 Idem Figure S1.2 for the model with 640k nodes.

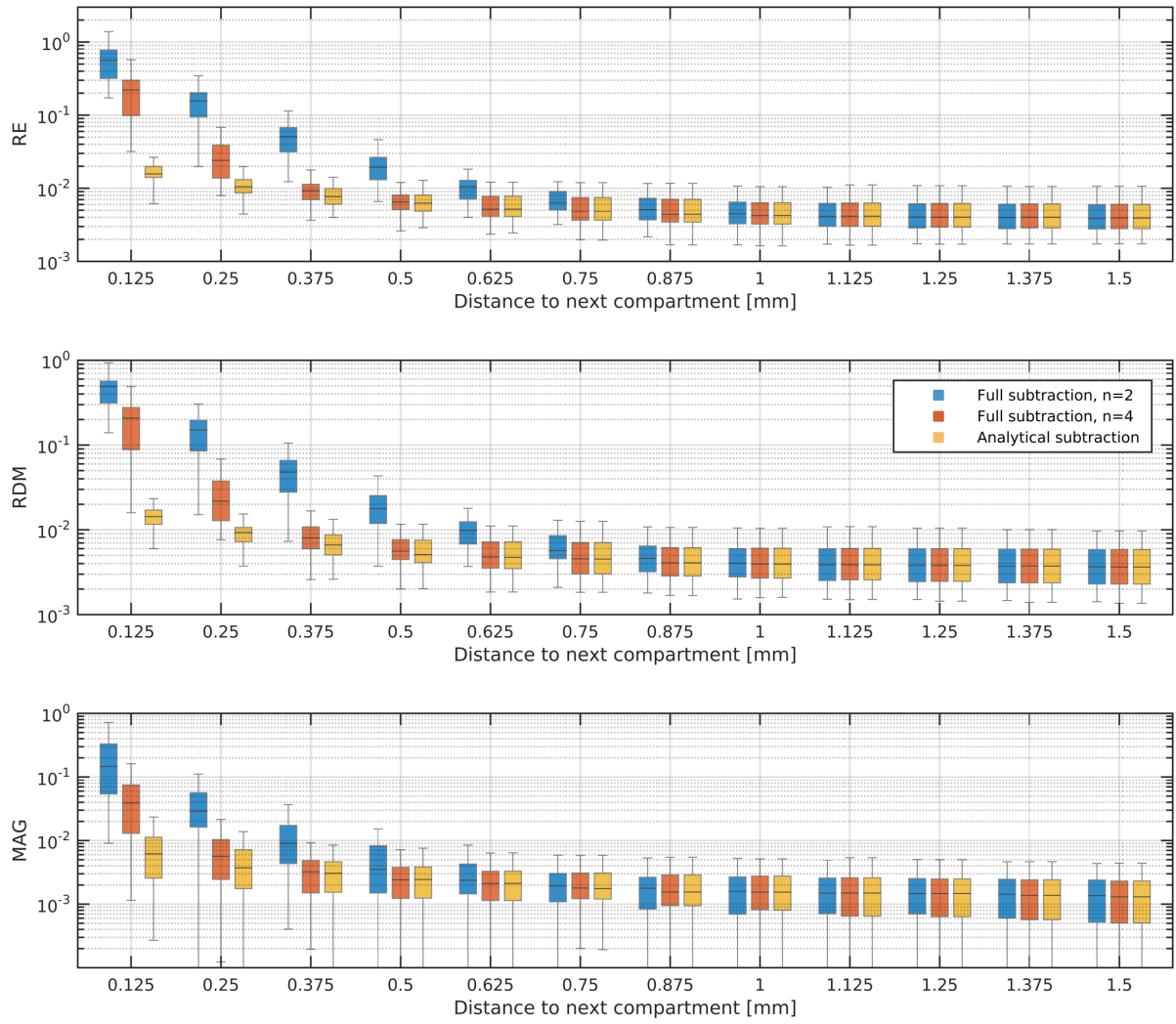


Figure S1.10 Idem Figure S1.3 for the model with 640k nodes.

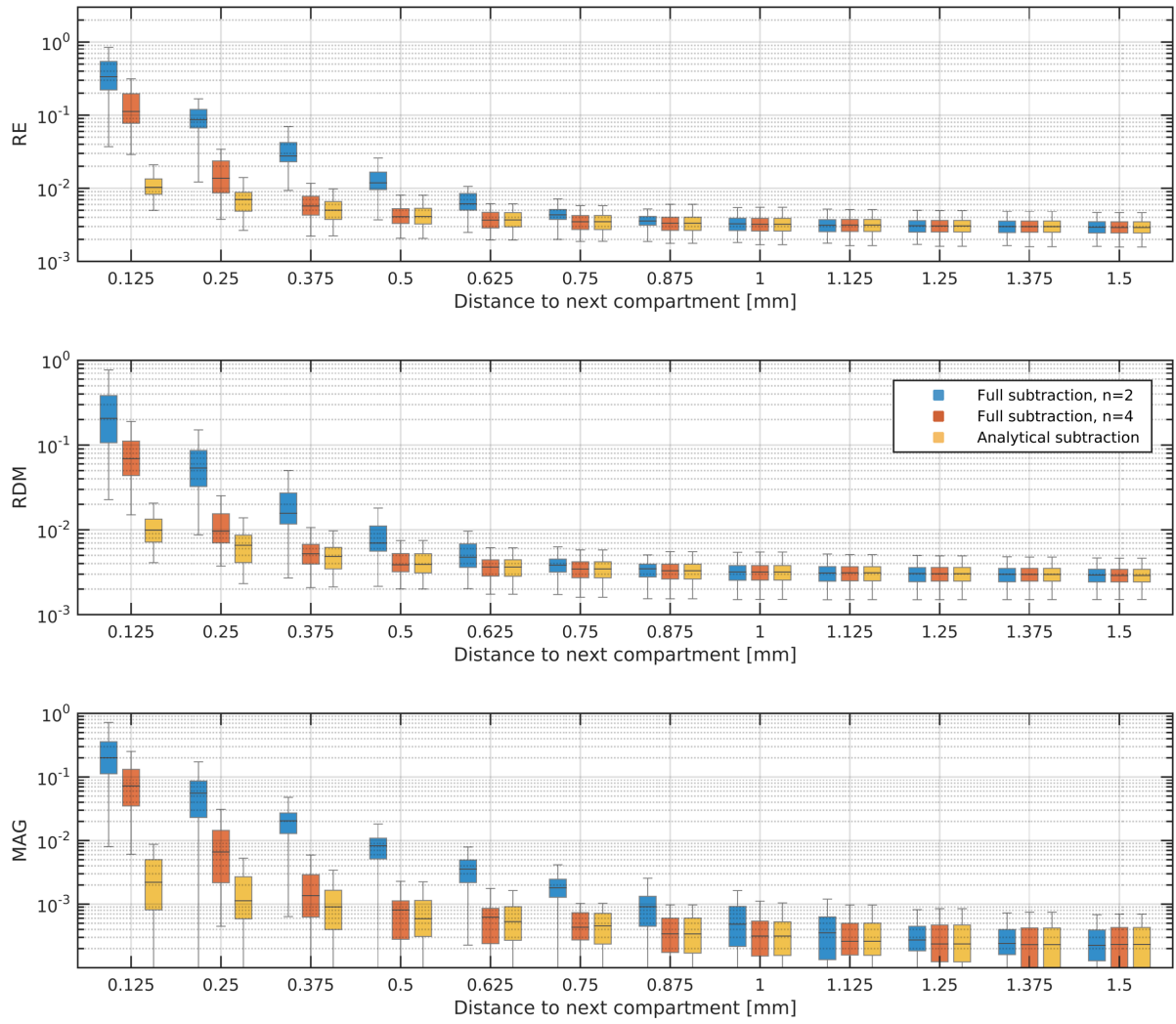


Figure S1.11 Idem Figure S1.2 for the model with 938k nodes.

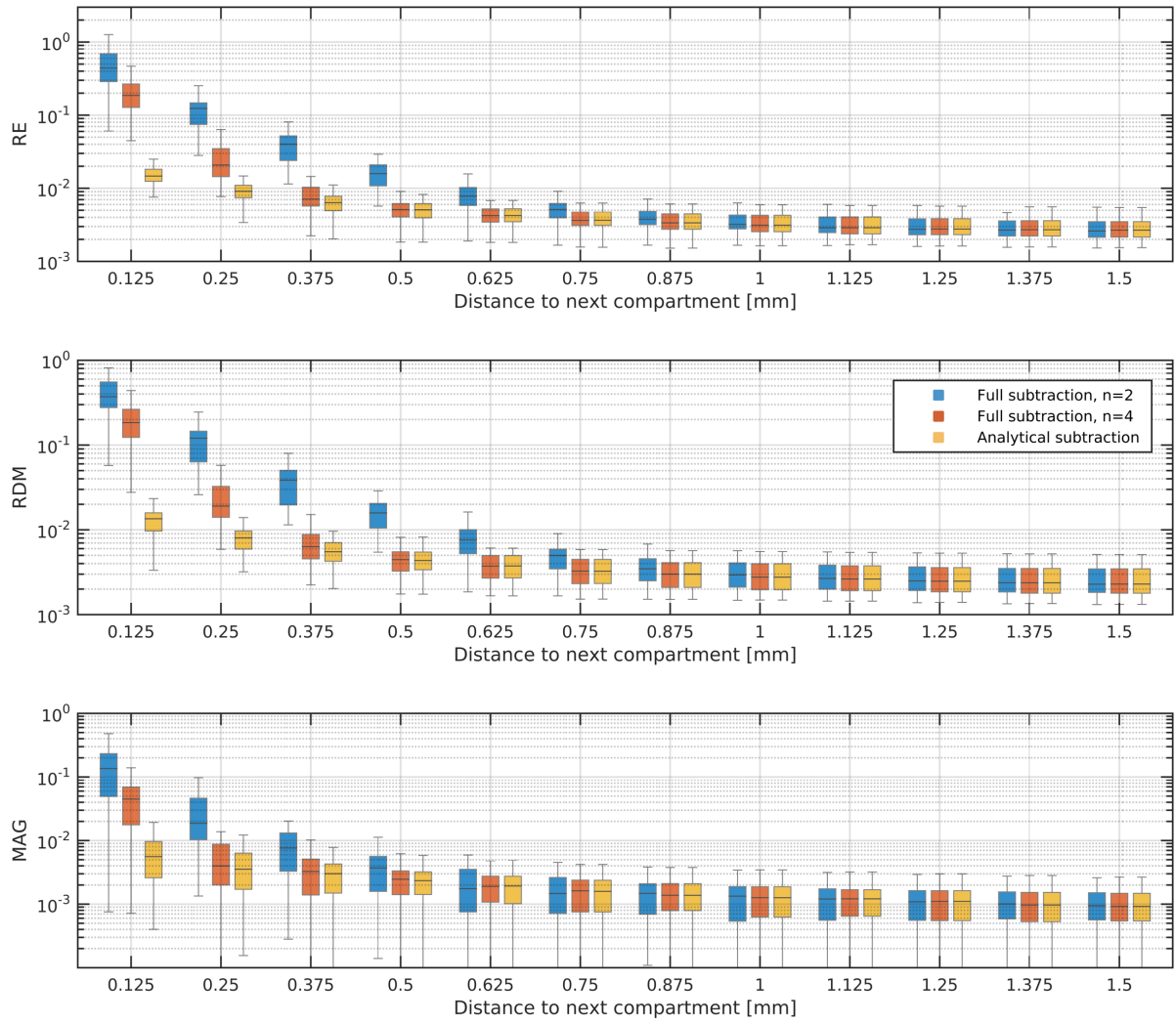


Figure S1.12 Idem Figure S1.3 for the model with 938k nodes.

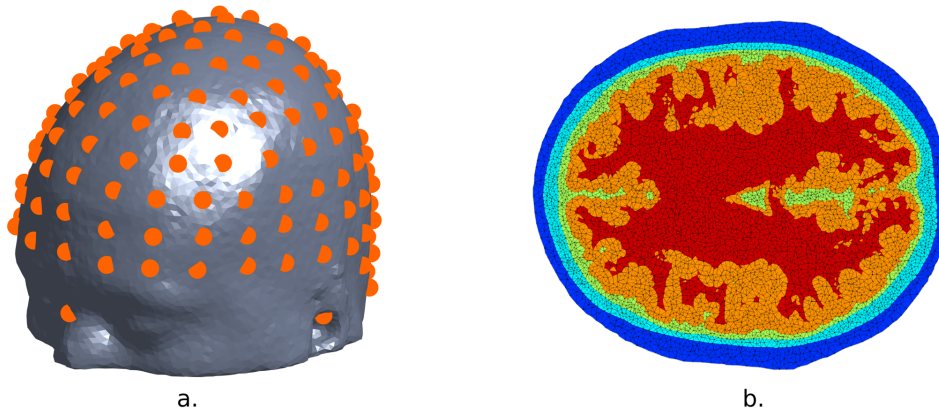


Figure S2.1 Details of the realistic head model utilised in the simulations. a. Scalp surface with the 162 electrodes placed according to the ABC standard. b. Cross section of the resulting tetrahedral mesh. Different tissue compartments are shown with different colours.

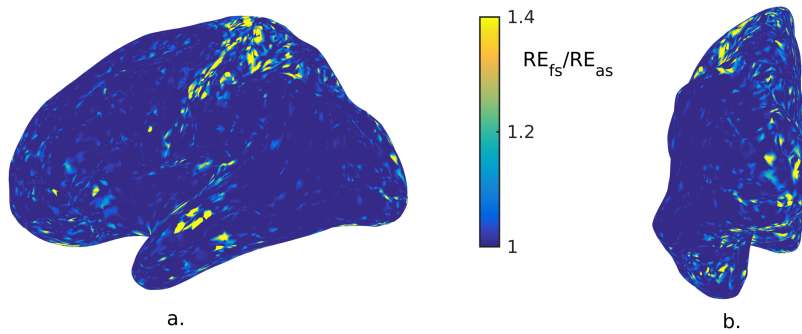


Figure S2.2 Ratio between the RE computed with the FS ($n=2$) and AS approaches (RE_{fs} and RE_{as} , respectively) utilising a model with 350k nodes obtained by coarsening the 600k nodes model (Figure S2.1). Solutions based on the AS method and the 600k nodes model were used as the reference. It can be seen that, although for most sources there is not a clear gain, it becomes significant for dipoles with $d/a \leq 0.5$ (see Figure 6.a-b). For these regions, the AS method provides solutions up to 60% more accurate (figure saturated for clarity). Results are presented from a lateral (a.) and anterior (b.) perspectives. It should be noted that, since the solution calculated with the 600k model is not free from errors, much caution should be taken for extracting conclusions.